ELSEVIER

Journal of Organometallic Chemistry 650 (2002) 210–222

Journal of Organometallic Chemistry

www.elsevier.com/locate/jorganchem

New studies on the apparent allyl rotation in scorpion-like palladium complexes. The influence of non-directly bonded groups. X-ray molecular structures of [Pd(η^3-2-Me-C_3H_4)L]TfO, L = bpzmArOMe and bpz*mCy

M. Carmen Carrión [a], Alberto Díaz [a], Ana Guerrero [a], Félix A. Jalón [a,*], Blanca R. Manzano [a], Ana Rodríguez [b], Rowena L. Paul [c], John C. Jeffery [c]

[a] *Dpt. de Quim. Inorg., Org. y Bioquim, Facultad de Químicas, Universidad de Castilla-La Mancha, Avda. Camilo J. Cela, 10, E-13071 Ciudad Real, Spain*

[b] *Escuela Técnica Superior de Ingeniería Industrial, Universidad de Castilla La Mancha, Avda. Camilo J. Cela, 3, E-13071 Ciudad Real, Spain*

[c] *The School of Chemistry, Cantock's Close, The University of Bristol, Bristol BS8 1TS, UK*

Received 1 December 2001; received in revised form 22 January 2002; accepted 22 January 2002

Abstract

New cationic 2-Me-allylpalladium complexes were prepared with the N,N-donor chelate ligands bis(pyrazol-1-yl)(R)methane (R = anisol-2-yl, bpzmArOMe; 2-hydroxyphenyl, bpzmArOH) and bis(3,5-dimethylpyrazol-1-yl)(R)methane (R = anisol-2-yl, bpz*mArOMe; cyclohexyl, bpz*mCy and ferrocenyl, bpz*mFc). The bpz′mR ligands adopt a rigid boat conformation after coordination to the Pd center and the R group is in the axial position of the metallacycle. The new complexes exhibit two isomeric forms in solution that differ in the relative orientation of the 2-Me-allyl group with respect to the bpz′mRPd fragment. The fluxional behavior of the new complexes, mainly in the context of the isomerization process, has been analyzed. Conclusions concerning the influence on this isomerization of the R group and the pyrazole substituents in positions 3 and 5 are discussed. The isomerization process was found to be affected by the presence of coordinating anions (Cl^-) or by a change in the complex concentration. The molecular structures of the complexes [Pd(η^3-2-Me-C_3H_4)(bpzmArOMe)]TfO and [Pd(η^3-2-Me-C_3H_4)(bpz*mCy)]TfO have been determined by X-ray diffraction studies.

Keywords: Palladium; Allyl; Bis(pyrazolyl); Rotation

1. Introduction

(η^3-Allyl)palladium complexes bearing N-donor ligands are very widely studied because they can act as precursors or intermediates in different catalytic processes [1]. Another aspect that has attracted a lot of interest in recent years is the study of the fluxional behavior in these systems, either directly related with the allyl group or with the ancillary ligands coordinated to the metal center [2]. For instance, in halophosphine [3], aminophosphine [4] and other Pd(II) derivatives [5] the allyl group frequently undergoes a mutual exchange of *syn* and *anti* protons, an interchange that is normally associated with a η^3–η^1–η^3 dynamic process. In several cases it has been demonstrated that this process is assisted by added base, the solvent, the counteranion [6] or a donor atom of an ancillary ligand [7]. The σ-donor character of phosphines or other donor ligands [5g] promotes easy access to the η^1-form of the coordinated allyl ligand, although steric effects have been shown to be important [5f]. In complexes bearing ligands with less σ-donor character a second dynamic process is more frequently observed, namely the apparent rotation of the allyl group [1k,8–10]. Depending on the molecular symmetry, this dynamic process is observed to occur via a *syn*–*syn*, *anti*–*anti* exchange or an isomerization process. One type of N,N-donor ligand that has been widely used in palladium chemistry is bis(pyrazol-1-yl)methane

* Corresponding author. Fax: +34-926-295318.
E-mail address: felix.jalon@uclm.es (F.A. Jalón).

0022-328X/02/$ - see front matter
PII: S0022-328X(02)01253-6

and its derivatives. This type of chelating ligand coordinates with the metal to form a six-membered metallacycle that adopts a boat conformation [11]. When hydrogen or methyl substituents [8a,12] are present in the spacer group situated between the pyrazole rings, the boat-to-boat interconversion usually takes place. It has been shown that the presence of two very different substituents in this spacer group makes the two boat conformations energetically very different [8g,13] and we have proposed that, as a consequence, the boat-to-boat interconversion is not present [8g,13a]. When methyl groups are present in the 3- and/or 5-positions of the pyrazole rings an enhancement of the rigidity of the boat conformation is also observed [8a]. In the work described here, which is mainly focused on the study of the apparent allyl rotation, we synthesized a number of new 2-Me-allyl palladium complexes with bis(pyrazol-1-yl)methane and bis(3,5-dimethylpyrazol-1-yl)-methane ligands. We chose N,N-ligands with only one bulky group in the spacer carbon (CHR) (see Scheme 1) for several reasons, (i) this would preclude the boat-to-boat interconversion process and, consequently, could simplify the study of the allyl rotation. (ii) As a consequence of the ligand rigidity, the two isomers generated in a situation of restricted allyl rotation would have very different chemical environments. (iii) The introduction of different R groups (and also methyl substituents in the pyrazole rings) would allow us to rationalize the effect that such groups have on the apparent allyl rotation and provide new data about the mechanism by which this process occurs.

2. Results and discussion

2.1. Synthesis of ligands and complexes

The ligands bis(pyrazol-1-yl)(R)methane (R = anisol-2-yl, bpzmArOMe; 2-hydroxyphenyl, bpzmArOH) and bis(3,5-dimethylpyrazol-1-yl)(R)methane (R = anisol-2-yl, bpz*mArOMe; cyclohexyl, bpz*mCy and ferrocenyl, bpz*mFc) were prepared by the reaction of 1,1′-carbonyldipyrazole (or the 3,5-dimethylpyrazole derivative) with the corresponding aldehyde in accordance with a previously described procedure (see Scheme 1) [14]. These ligands are soluble in organic solvents such as diethyl ether or more polar solvents. The Me-allylPd complexes were prepared by treatment of the dimer $[Pd(\eta^3\text{-}2\text{-}Me\text{-}C_3H_4)(\mu\text{-}Cl)]_2$ with $AgCF_3SO_3$ (AgTfO) in solution in THF. The AgCl formed in the reaction was filtered off and the corresponding bpz′mR ligand was subsequently added. The reaction is represented in eq. 1.

$$1/2[Pd(\eta^3\text{-}C_4H_7)(\mu\text{-}Cl)]_2 + AgTfO \rightarrow [Pd(\eta^3\text{-}C_4H_7)(S)_2]TfO \xrightarrow{bpz'mR} [Pd(\eta^3\text{-}C_4H_7) \times (bpz'mR)]TfO \quad (1)$$

pz′ = pz, R = 2-OH-C_6H_4 (**1**), 2-OMe-C_6H_4 (**2**). pz′ = 3,5-Me_2pz = pz*, R = 2-OH-C_6H_4 (**3**), 2-OMe-C_6H_4 (**4**), Cy (**5**), Fc (**6**).

Complexes **2** and **4**–**6** are soluble in acetone, THF and more polar organic solvents. Complexes **1** and **3** are sparingly soluble in these solvents.

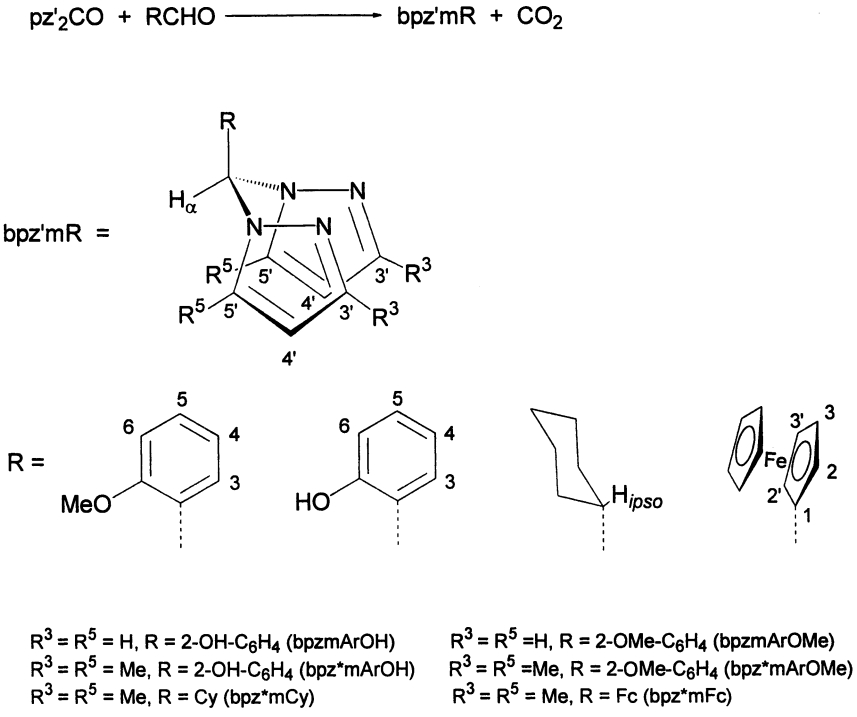

Scheme 1.

2.2. Characterization of the new complexes

Complexes **1**–**6** were characterized by NMR and IR spectroscopy and elemental analysis. The IR spectra show the characteristic vibration bands of the 2-Me-allyl group, the pyrazole groups, the counter anion ($CF_3SO_3^-$) and also those of the R substituents (see Section 4).

The ^1H and ^{13}C-NMR data of complexes **1**–**6** are compiled in Tables 1 and 2, respectively. Assignment of the different resonances was made by considering the chemical shifts and coupling constants expected for the different atoms and the information obtained from ^1H–^1H COSY experiments. NOE studies, which will be discussed later, were of significant value in terms of complementary assignment information.

Evidence for complexation of the bpz′mR ligands in the final compounds is provided by the observation of positive coordination-induced shifts (CIS) for the pyrazolyl atoms, the interpyrazolic CH_α fragment and several protons of the R groups when compared with those of the free ligands. Some NOEs observed ($H^{3'}$ or Me^3 with H_{syn} or H_{anti}; phenylic H^3 in **1**–**4** or H^2 in **6** with H_α) also reflected the coordination of the ligands and/or supported the signal assignments. For the whole set of complexes an NOE between $H^{5'}$ (or Me^5) and H_α was observed but such an interaction was not observed for protons of the R group (see Scheme 2). From these data it is possible to conclude that the R group is in an axial position (form A, Scheme 2) and form B is unpopulated. The positioning of the relatively bulky fragment R (when compared with H) in an equatorial position must cause steric repulsion with Me^5 and even with the $H^{5'}$ pyrazolic groups. Other authors have also suggested the axial position of the R group in similar systems [8g,13]. A low temperature spectrum (213 K) was recorded for some complexes (**4** and **5**) and, in these cases, splitting of the signals was not observed. Consequently, as we have observed previously for other bis(pyrazolyl)methane complexes with R substituents in the spacer group [8g,13a], the boat-to-boat interconversion does not occur and the ligand is a rigid system after coordination. The axial orientation of the R group on the CH_α fragment confers on the PdbpzmR moiety a characteristic aspect of a trapped metal in the claws of a tailed ligand, a situation that inspired us to term these ligands 'scorpion-like' in a similar way to Trofimenko's scorpionates [15].

All the complexes showed the presence of two diastereomers in solution at room temperature and these differ in the relative orientation of the allyl group with respect to the PdNN fragment (*endo* and *exo* isomers) (see Scheme 3). Comparable behavior has been observed in similar complexes [8a,8g,16]. We propose that in our case the separate observation of these isomeric forms is possible (discussed below) due to the restricted rotation of the allyl group. For each complex the corresponding diastereomers are in solution in a ratio that depends on the solvent, reflecting the fact that the two isomers are in equilibrium. By considering the data of different NOE experiments it was possible to elucidate the structure of each specific isomer. For the *exo* isomers the most informative interaction was the NOE observed between the allylic methyl group and protons of the R group or that between the H_{anti} and the Me^3 of the pyrazole ring (see Scheme 2). A noticeable characteristic of the spectra is the shielding produced on the Me-allyl groups in the *exo* isomers when the R group contains an aromatic ring, a situation probably induced by the electron current anisotropy. This effect has also been observed for the complex [2-Me-allylPd(bpz*mPh)]TfO, **7** [8g]. We found that the major isomer corresponds to the *exo* form. The only exception occurs for complex **2**, whose isomers are ca. in a 1:1 ratio in chloroform-*d*. However, in other solvents, such as acetone-d_6 or 1,1′,2,2′-tetrachloroethane-d_2, the *exo* form is the major component of the mixture.

2.3. Rotation and most stable conformation of the R group

As we have previously observed in other related scorpion-like complexes with aromatic R groups, e.g. complex **7** [8g], the phenylic H^3 (**1**–**4**) or the ferrocenyl H^2 (**6**) protons show a negative CIS when compared with the free ligands. This CIS can be explained by the fact that, although the R groups can rotate around the R–C_α bond, there are preferred conformations that result in an overall shielding effect due to the electron current anisotropy of the pyrazole rings. The conformations shown in Scheme 4 are those found in different X-ray structures of complexes containing these ligands [8g,13a] (see below for the X-ray structures of complexes **2** and **5**) and are in accordance with the observed shielding (A–C in Scheme 4). In contrast, a positive CIS is observed for the H_{ipso} proton of the Cy fragment in **5**. This proton shows a $^3J_{HH}$ coupling constant with H_α of 11 Hz, which is characteristic of a mutual *axial–axial* disposition of the two protons. Both of these facts point to a preferred conformation in which the C–H_{ipso} bond is contained in the mirror plane of the complex (see Scheme 4(D)).

VT NMR experiments were carried out in 1,1′,2,2′-tetrachloroethane-d_2 for the major isomers of complexes **2**, **4**–**6** and **7** (previously reported [8g]) between 293 K and the coalescence temperature of the corresponding rotamers (320–373 K). A measure of the evolution of the chemical shift with temperature of the protons assigned that could be affected by the pyrazolic electron current anisotropy (H^3 and OMe for the anisole derivatives **2** and **4**, *ortho*-protons for **7**, H^2–Fc for **5** and H_{ipso}–Cy for **6**) was undertaken. These resonances

Table 1
^{1}H-NMR data for complexes **1**–**6** at room temperature

Complex	Pyrazole			H_α	R group	Allyl–Pd		
	$H^{4'}$	$H^{3'}$ or Me^3	$H^{5'}$ or Me^5			H_{syn}	H_{anti}	Me
1M (73%)	6.67(t)	8.11 (d,$J_{34}=2.2$)	8.52 (dd,$J_{45}=2.6$, $J_{35}=0.73$)	8.59	6.95(d, H^6, $J_{56}=8.1$, 7.03(t,H^4, $J_{45}=8.0$), 7.27(t, H^5), 7.27 (d, H^3, $J_{34}=8.3$), 9.30(s, OH)	4.13	3.33	1.98
1m [a]	6.65(t)	[b]	[b]	8.64	6.92(d), 7.31(t)	4.32	2.94	2.27
2M (57%)	6.43(t)	7.70(bs)	8.49(d) $J_{45}=2.7$	8.54	6.84(d, H^6, $J_{56}=8.3$), 6.79(t,H^4, $J_{45}=7.6$), 7.31(t, H^5), 6.62 (d, H^3, $J_{34}=7.6$), 3.71(s, OMe)	3.88	3.10	2.17
2m	[b]	[b]	[b]	[b]	[b]	4.06	2.92	1.85
3M (66%)	6.06	2.28	2.49	7.36	6.25(bd, H^6), 7.20 (m, H^4), 7.20(m, H^5), 6.66 (bs, H^3), 9.05(s, OH)	3.87	2.95	1.51
3m	6.06	2.20	2.51	7.48	6.56(bd, H^6), 7.20 (m, H^4), 7.20(m, H^5), 6.66 (bs, H^3), 9.05(s, OH)	4.00	2.41	2.19
4M (65%)	6.14	2.32	2.55	7.46	6.91(d, H^6, $J_{56}=8.1$), 6.90 (m, H^4), 7.38(t, H^5), 6.48 (d, H^3, $J_{34}=7.3$), 3.70(s, OMe)	3.90	3.05	1.54
4m	6.12	2.22	2.60	7.63	3.71(s, OMe)	4.04	2.16	2.19
5M [c]	6.03	2.31	2.51	6.12 (d, $J_{HH}=11.0$)	3.4(qt, CH_{ipso})	4.16	3.18	2.22
6M (66%)	6.16	2.28	2.65	7.74	4.25(Cp), 3.90(H^2, $H^{2'}$), 4.19(H^3, $H^{3'}$)	3.85	3.02	1.65
6m	6.13	2.19	2.68	7.74	4.31(Cp), 4.02(H^2, $H^{2'}$), 4.22(H^3, $H^{3'}$)	4.01	2.26	2.16

See Scheme 1 for numbering. Chemical shifts in ppm and coupling constants in Hz. All resonances are singlets if not specified. The percentage of the major isomer is indicated between parenthesis. d, doublet, t, triplet, m, multiplet, bs, broad singlet, q, quartet. M and m, major and minor isomers, respectively. Solvent is chloroform-*d* if not specified.

[a] In acetone-d_6.

[b] Resonances non observed.

[c] Signals for **5m** are not clearly observed.

Table 2
$^{13}C\{^1H\}$-NMR data for complexes **1**–**6** at room temperature

Complex	Pyrazole				C_α	R group	Allyl–Pd		
	$C^{4'}$	$C^{3'}$	$C^{5'}$	Me^3 and Me^5			CH_2=	=C–	Me
1M [a]	107.61	146.27	136.08			155.65, 122.35, 116.77, 120.03, 131.93, 127.64	72.98		
1m [a]	107.61	146.75	136.14			116.95, 120.03, 132.28, 127.85	73.24		
2M	106.76	144.38	135.97	–	71.75	157.10, 123.09, 111.44, 119.53, 131.21, 126.54, 55.55(OMe)	59.53	133.61	23.02
2m	106.76	144.85	136.10	–	72.07	157.30, 122.85, 111.60, 119.53, 131.61, 126.88, 55.57(OMe)	59.55	133.75	23.53
4M	107.89	153.05	143.89	15.48 12.05	66.56	122.87, 128.11, 121.15, 132.04, 112.27, 59.79(OMe)	56.3(bs)	132.47	23.16
4m	107.53	152.33	144.22	15.81 12.05	67.03	128.83, 119.92, 132.69, 112.40, 60.21 (OMe)	56.3(bs)		23.42
5M	107.21	152.09	143.67	15.04 11.55	71.65	44.31, 25.12, 27.46, 25.12	60.04	131.10	23.85
6M	107.75	152.80	142.16	14.97 11.61	68.46	69.65(Cp), 68.85, 67.45, 82.65(C^1)	59.10	132.00	23.30
6m	107.40	152.25	142.53	15.29 11.61	67.80	69.52(Cp), 68.75, 67.60, 82.32(C^1)	60.06	130.50	23.00

See Scheme 1 for numbering. Chemical shifts in ppm. All signals are singlets. bs, broad singlet. M and m, major and minor isomers, respectively. Solvent is chloroform-*d* if not specified.
[a] In acetone-d_6.

did not change significantly in the phenylic compounds whereas a clear decrease in the absolute value of the corresponding CIS with increasing temperature was observed for complexes bearing Cy (**5**) or Fc (**6**) groups. Considering the rigidity and structural analogy of this set of complexes, the comparable region of studied temperatures and the identical solvent, we propose that this evolution of chemical shifts for complexes **5** and **6** is related to an increase in the population of the excited rotational states of the R groups. In accordance with these observations, the fundamental state (more populated rotamer at r.t) for **5** and **6** must correspond to the less sterically demanding disposition of the R groups (see Scheme 4(D and C)). In this disposition the H^2–Fc and H_{ipso}–Cy are inside and outside, respectively, of the shielding electron current anisotropy of the pyrazoles. Other conformations for the R group would be less populated at r.t. and begin to be more populated as the temperature increased. As a consequence, the H^2–Fc experiences the observed deshielding while the H_{ipso}–Cy experiences the aforementioned shielding. We can conclude that the rotational barrier for the more bulky groups, Cy and Fc is higher than for R-phenyl groups. For these last R-groups the barrier is clearly overcome at r.t.

2.4. Isomer interconversion. Apparent allyl rotation

As we have previously stated, two isomers (see Scheme 3) were observed for complexes **1**–**6** (and also for **7**) that differ in the relative orientation of the allyl group with respect to the Pd-NN ligand backbone. The NOE experiments carried out at r.t. indicate that the isomer interconversion does take place. For instance, when the allyl Me group of one isomer is irradiated, high magnetization transfer is observed on the same group of the second isomer as a consequence of the spin relaxation. Even more informative is the fact that an intense magnetization transfer is observed between H_{syn} (or H_{anti}) protons of one isomer with those of the other, but not between H_{syn} and H_{anti} protons. The existence of H_{syn}–H_{syn} (and H_{anti}–H_{anti}) and not H_{syn}–H_{anti} exchange clearly indicates that the isomerization phenomenon is related to an apparent allyl rotation and not with a η^3–η^1–η^3 pathway. Given the intensity of the magnetization transfer at room temperature, we decided to study the isomerization process by determining the coalescence temperatures and to analyze the influence of the Me pyrazolic substituents and the R group of the N,N-donor ligands. The corresponding VT ^{1}H-NMR studies were recorded for the more soluble complexes **2**

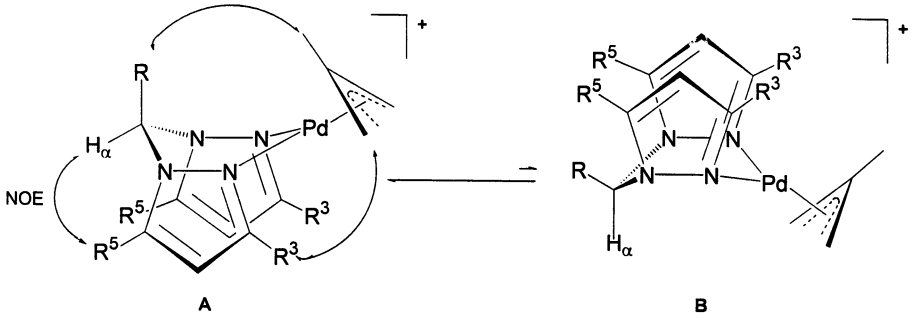

Scheme 2.

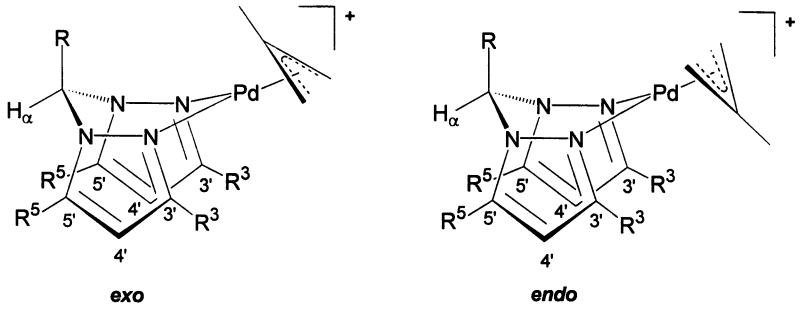

Scheme 3.

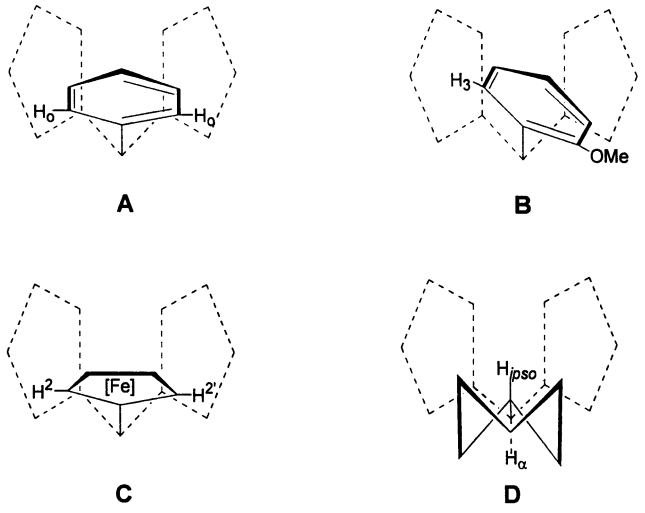

Scheme 4.

and **4**–**7** in 1,1′,2,2′-tetrachloroethane-d_2. In order to exclude the influence of other variables, similar molar concentrations in the same solvent and with the same counteranion ($CF_3SO_3^-$) were used for all the complexes. Coalescence temperatures were achieved in the range 299–391 K. The corresponding $\Delta G_c^{\ddagger}$ data are compiled in Table 3 and represented in Fig. 1. The $\Delta G_c^{\ddagger}$ values fit straight lines with, in general, very low slopes. Exceptionally, for **6** the line has a clear positive slope. Complex **4** exhibits slightly higher values than complex **2**, which suggests that the Me substituents in the pyrazole rings make the isomerization process more difficult, although not markedly so. A more marked influence of the R groups can be seen when values for complexes **4**–**7** are compared. Cy and Ph groups in complexes **5** and **7**, respectively, induce similar energetic barriers. However, the introduction of a methoxy group in complex **4** gives rise to a remarkable increase in this barrier.

The effect of the concentration and the addition of a counteranion with coordination ability (Cl^-) was also analyzed in the case of **4**. This study was performed by the addition of more solvent (1,1′,2,2′-tetrachloroethane-d_2) and PPh_4Cl, respectively, to solutions of the complex. The dilution produced an increase and the addition of chloride a decrease in the $\Delta G_c^{\ddagger}$ values (see Table 3 and Fig. 2). The favorable effect on the isomerization in Pd(II) complexes of coordinating agents (through pentacoordinate [9] or tricoordinate [10] intermediates) such as solvent, counteranions or internal functional groups in the ligands is widely reported and, consequently, the effect of the chloride ion is not unexpected. Both experiments on complex **4** could lead to a perturbation in the counteranion–cation contact that would explain the observed behavior. The dilution would make this contact more difficult (ion-pair dissociation) while the addition of anions with more coordinating ability (Cl^- vs. TfO^-) would improve this contact.

An acceleration in the process would be expected when coordinative functional groups are present in the R fragments of the ligands, such as OMe in **4**. Complex **4**, however, exhibits the highest $\Delta G_c^{\ddagger}$ values (Fig. 1). On the basis of these data it is possible to conclude that the OMe group does not participate in the stabilization of any intermediate. This conclusion excludes the formation, through a Pd–N bond rupture, of tricoordinated intermediates where an interaction with the OMe group may be feasible. After considering the experimental data as a whole, we propose that for our complexes the anion–cation interaction is the main cause of the isomerization process through a pentacoordinated intermediate. The orbital perpendicular to the coordination plane of the complex must be the direction in which this interaction occurs. For complexes with phenylic-R groups containing the MeO substituent (**2** and **4**), this contact could be hindered by virtue of the orbital being blocked. Such orbital blocking would be more pronounced for complex **4**, which also has Me substituents in the pyrazole rings. Bulky groups such as Cy and Fc must have a very different effect when they are oriented away or towards the palladium centre. In accordance with the $\Delta G_c^{\ddagger}$ data, the Cy group in **5** is not very effective in blocking the palladium centre, probably due to the different skeletal conformations that this group can adopt—even in a regime of free rotation that would move this group away from the allyl–Pd moiety. In contrast, the Fc group in **6** is rigid and there will be orientations of this group that will severely hinder the

Table 3
Free energies of activation at the coalescence temperatures for the isomerization process in complexes **2**, **4**–**7** in 1,1′,2,2′-tetrachloroethane-d_2

Complex	Exchanging group	$\Delta G_c^{\ddagger}$/kJ mol^{-1} (T/K)	Complex	Exchanging group	$\Delta G_c^{\ddagger}$/kJ mol^{-1} (T/K)
7	Me^5	66.2 (305)	**2**	OMe	76.8 (337)
7	Me^3	67.0 (315)	**2**	H_{syn}	77.4 (353)
7	H_{syn}	66.6 (323)	**2**	$H^3_{anisole}$	77.3 (363)
7	H_{orto}	66.8 (325)	**2**	Me_{allyl}	77.6 (385)
7	Me_{allyl}	66.2 (343)	**4**	Me^5	81.1 (361)
5	Me^5	66.5 (299)	**4**	Me^3	81.0 (369)
5	Me^3	67.8 (315)	**4**	H_{syn}	81.8 (383)
5	H_{syn}	67.1 (321)	**4**	$H^3_{anisole}$	81.7 (391)
5	H_{α}	67.2 (321)	**4** dilution	Me^5	86.0 (391)
5	H_{anti}	67.6 (327)	**4** dilution	Me^3	87.1 (407)
5	H_{ipso}	67.2 (339)	**4**+PPh_4Cl	Me^5	71.4 (327)
6	H_{α}	74.8 (325)	**4**+PPh_4Cl	Me^3	72.0 (339)
6	Me^5	76.1 (333)	**4**+PPh_4Cl	H_{syn}	72.6 (349)
6	$H^{4'}$	77.2 (345)	**4**+PPh_4Cl	$H^3_{anisole}$	72.8 (363)
6	Me^3	80.5 (375)			
6	H_{syn}	81.0 (385)			

Values are represented vs. temperature in Figs. 1 and 2. Values have been calculated in accordance with the Shanan-Atidi and Bar-Eli [21] method for the exchange of the minor to the major isomers.

cation–anion interaction. As stated previously, as the temperature is increased the populations of the rotational states that cause greater steric hindrance, which could also hinder the cation–anion contact, are also increased. In accordance with this hypothesis the $\Delta G_c^{\ddagger}$ values for **6** quickly increase with temperature.

2.5. X-ray structures of complexes 2 and 5

Crystals of **2** and **5** belong to the monoclinic (*C*2/c) and orthorhombic (*Pnma*) space groups, respectively. The molecular structures consist of a mononuclear Pd cation and a triflate counteranion. ORTEP plots of the cations are shown in Figs. 3 and 4. The crystallographic data and a list of selected bond distances and angles are given in Tables 4 and 5, respectively. In complex **5**, the cation lies on a crystallographic mirror plane containing Pd(1), C(12), C(13) and C(7). In both compounds the geometry around the Pd(1) atom is ca. square-planar with two coordinated pyrazole rings and the η^3-bonded allyl ligand. The distances of the Pd(1)–N coordination bonds are comparable to those of other bispyrazolyl-

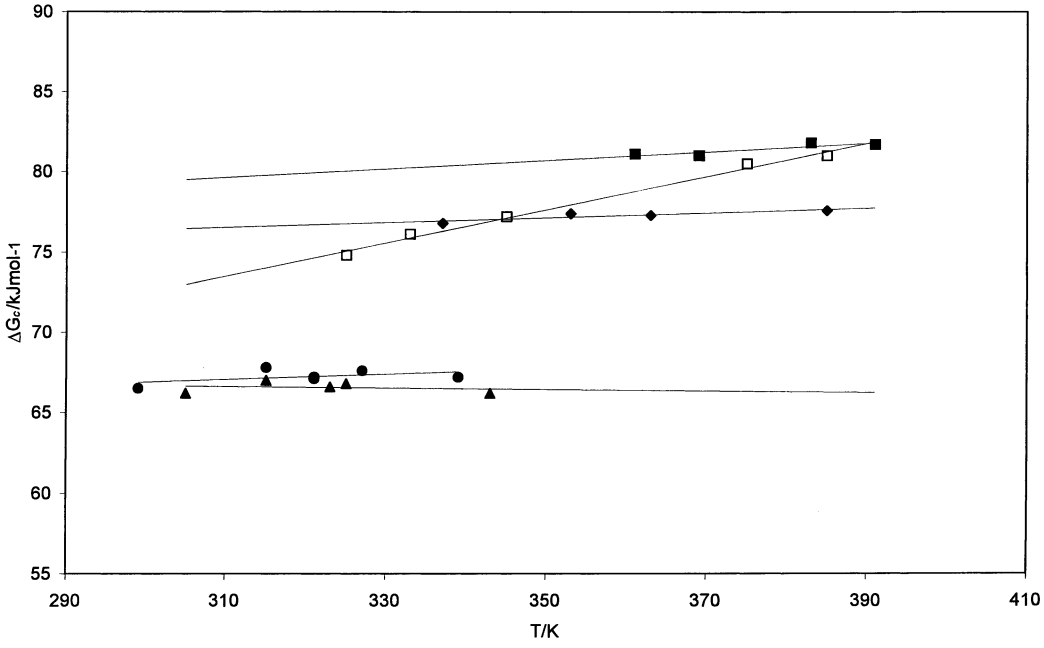

Fig. 1. Linear plot of $\Delta G_c^{\ddagger}$ (kJ mol^{-1}) vs. T_c for the isomerization process of [Pd(η^3-C_4H_7)(bpz′mR)]TfO complexes in 1,1′,2,2′-tetrachloroethane-d_2 (see Table 3 for values): (▲) **7** (●) **5** (◆) **2** (■) **4** (□) **6**.

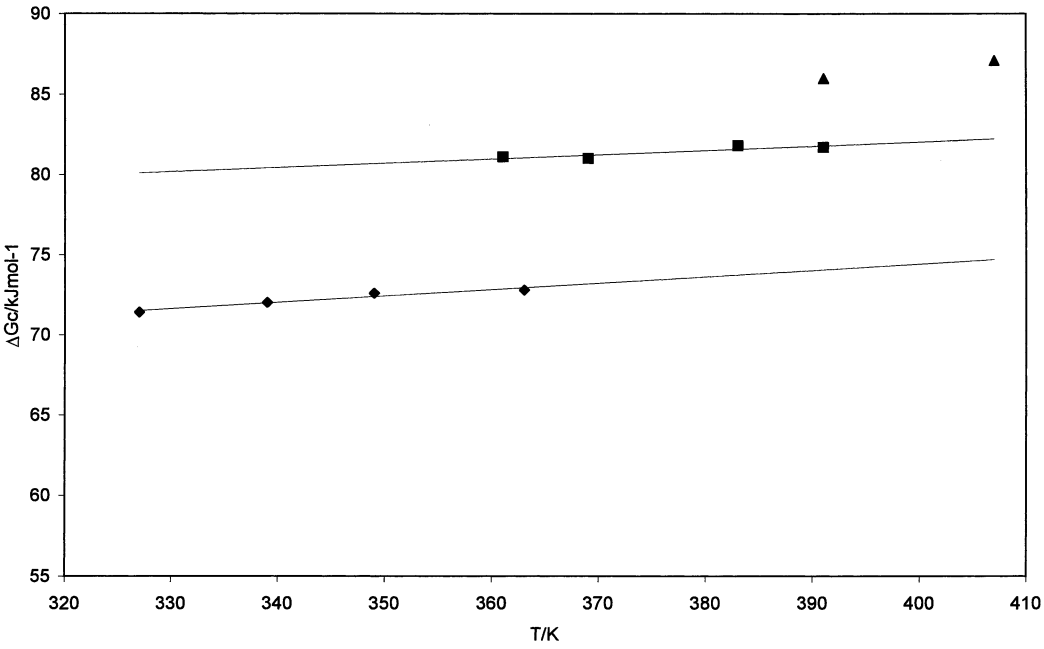

Fig. 2. Linear plot of $\Delta G_c^{\ddagger}$ (kJ mol^{-1}) vs. T_c for the isomerization process of complex **4** in 1,1′,2,2′-tetrachloroethane-d_2: (■) 1.6×10^{-2} mol l^{-1} (▲) 0.8×10^{-2} mol l^{-1} (◆) Addition of 5.14 mg of PPh_4Cl (1.37×10^{-2} mmol) to 0.50 ml of the 1.6×10^{-2} mol l^{-1} solution of complex **4**.

methane [8g,12b,17] complexes. The coordination of the bpz′mR ligand gives rise to a boat-like metallacycle, PdNNCNN, with the anisole (**2**) or cyclohexyl (**5**) group attached to the carbon atom in an axial orientation. This situation is in agreement with the data obtained for the complexes in solution. In complex **2** the anisole plane is twisted (62.60°) with respect to the plane defined by the Pd(1)–C(11)–C(12) atoms. The OMe group lies practically in the anisole plane and points away from the molecule. On the contrary, the cyclohexyl group in **5** is bisected by the previously mentioned crystallographic plane. It has been described that the steric hindrance between the C^3 substituents of the pyrazole and the ancillary ligands bonded to Pd promotes several distortions [17a]. In our case, comparing complexes **2** and **5**, we have found that the methyl groups in this position induce the following distortions in the boat metallacycle, (i) The dihedral angle PdNN/NNNN is smaller in **5** (153.59°) than in **2** (157.7°) which reduces the steric hindrance. (ii) As a consequence, the dihedral angle between the two pyrazole rings is smaller for **5** (124.18°) than for **2** (128.3°). (iii) The same steric repulsion influences the NPdN bite angle, which is slightly less open in **5** [87.4(1)°] than in **2** [88.4(8)°].

In complex **5** the isomer found in the solid state is the *exo* form and this corresponds with the major isomer

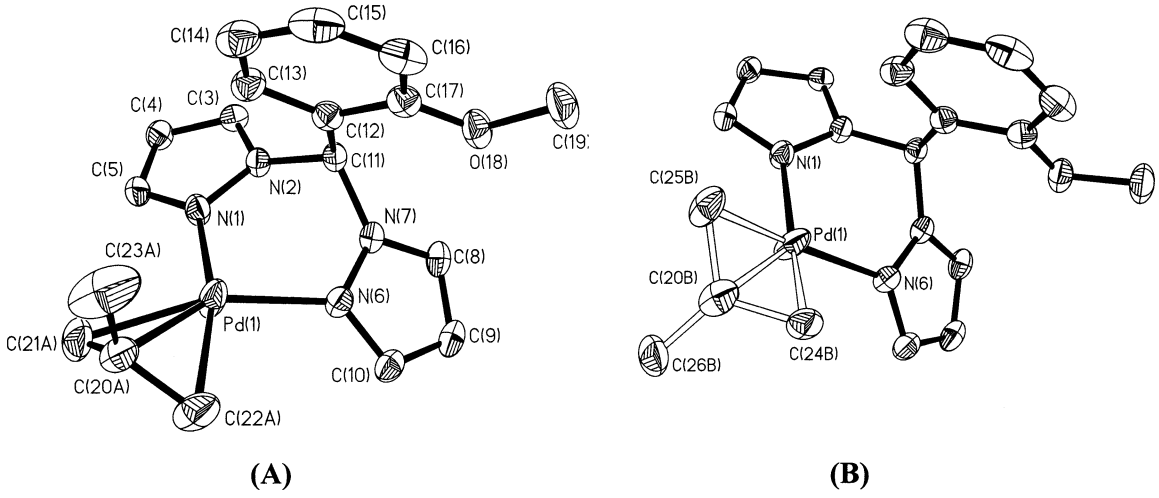

Fig. 3. ORTEP view with atomic numbering of the cation of the two isomers (*exo*, A and *endo*, B) of **2** (40% probability ellipsoids). Proton atoms have been omitted for clarity.

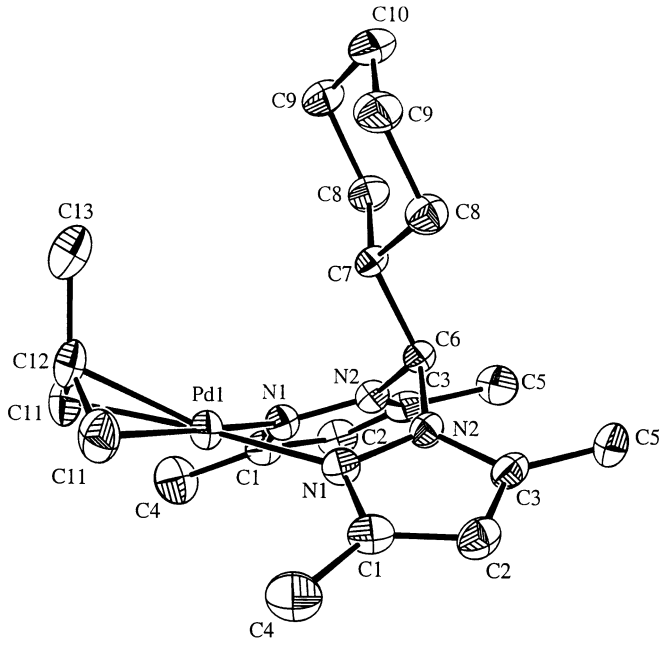

Fig. 4. ORTEP view with atomic numbering of the cation of **5** (30% probability ellipsoids). Proton atoms have been omitted for clarity.

Table 4
Crystal data and structure refinement for **2** and **5**

	2	**5**
Empirical formula	$C_{19}H_{21}F_3N_4O_4PdS$	$C_{11}H_{16.5}F_{1.5}N_2O_{1.5}Pd_{0.5}S_{0.5}$
Formula weight	564.86	298.49
Temperature (K)	173(3)	293(2)
Wavelength (Å)	0.71073	0.71070
Crystal system	Monoclinic	Orthorhombic
Space group	*C2/c*	*Pnma*
a (Å)	17.295(2)	16.276(5)
b (Å)	11.1775(13)	10.441(3)
c (Å)	23.205(3)	15.420(2)
Volume (Å^3)	4454.1(9)	2620.4(12)
Z	8	8
D_{calc} (g cm^{-3})	1.685	1.513
Absorption coefficient (cm^{-1})	0.985	0.839
F(000)	2272	1224
Crystal size (mm)	0.3 × 0.3 × 0.3	0.4 × 0.3 × 0.2
Limiting indices	$-22 \le h \le 22$, $-9 \le k \le 14$, $-29 \le l \le 29$	$0 \le h \le 21$, $0 \le k \le 13$, $0 \le l \le 20$
Data/restraints/parameters	5101/13/328	3332/0/184
Goodness-of-fit on F^2	1.033	0.988
Final *R* indices [$I > 2\sigma(I)$]	$R_1 = 0.0353$, $wR_2 = 0.0844$	$R_1 = 0.0355$, $wR_2 = 0.0896$
R indices (all data)	$R_1 = 0.0514$, $wR_2 = 0.0906$	$R_1 = 0.0584$, $wR_2 = 0.1070$
Largest difference peak and hole (e Å^{-3})	0.745 and −2.145	0.821 and −0.560

Table 5
Selected bond lengths (Å) and angles (°) for **2** and **5**

2

Bond lengths		*Bond angles*	
Pd(1)–N(1)	2.100(2)	N(6)–Pd(1)–N(1)	88.4(8)
Pd(1)–N(6)	2.085(2)	C(21A)–Pd(1)–C(22A)	67.4(8)
Pd(1)–C(21A)	2.195(2)	C(24B)–Pd(1)–C(25B)	67.9(8)
Pd(1)–C(22A)	2.112(2)	C(21A)–Pd(1)–N(1)	98.3(8)
Pd(1)–C(20A)	2.125(2)	C(25B)–Pd(1)–N(1)	102.3(8)
C(20A)–C(21A)	1.430(10)	C(22A)–Pd(1)–N(6)	103.2(8)
C(20A)–C(22A)	1.425(9)	C(24B)–Pd(1)–N(6)	100.0(8)
C(20A)–C(23A)	1.454(10)	C(21A)–C(20A)–C(22A)	113.6(7)
Pd(1)–C(20B)	2.092(2)	C(25B)–C(20B)–C(24B)	112.9(7)
Pd(1)–C(24B)	2.166(2)	N(2)–C(11)–N(7)	109.0(2)
Pd(1)–C(25B)	2.159(2)	C(17)–O(18)–C(19)	117.8(3)
C(20B)–C(24B)	1.426(10)		
C(20B)–C(25B)	1.435(10)		
C(20B)–C(26B)	1.450(10)		
N(1)––N(2)	1.361(3)		
N(6)–N(7)	1.357(3)		
N(2)–C(11)	1.463(3)		
N(7)–C(11)	1.463(3)		
C(11)–C(12)	1.520(4)		
O(18)–C(17)	1.366(3)		
O(18)–C(19)	1.434(3)		

5

Bond lengths		*Bond angles*	
Pd(1)–N(1)	2.110(2)	N(1)–Pd(1)–N(1)	87.36(13)
Pd(1)–C(11)	2.109(3)	C(11)–Pd(1)–C(11)	68.3(2)
Pd(1)–C(12)	2.119(4)	C(11)–Pd(1)–N(1)	170.34(12)
C(6)–N(2)	1.458(3)	C(11)–C(12)–C(11)	114.6(5)
C(6)–C(7)	1.527(5)	N(2)–C(6)–N(2)	109.4(3)
N(1)–N(2)	1.371(3)	N(2)–N(1)–Pd(1)	120.04(17)
C(12)–C(11)	1.407(5)	N(1)–N(2)–C(6)	119.9(2)
C(12)–C(13)	1.489(8)		

found in solution. If we define a plane containing the Pd and the two coordinated nitrogen atoms, then the terminal allylic carbons are situated 0.064 Å below this plane and the central allylic carbon is 0.644 Å above it. The plane of the allyl group defines an angle of 111.1° with the coordination plane in such a way that the C(central) to $-CH_3$ vector is pointing away from the metal.

Interestingly, both isomers of complex **2** are present in the crystal. The allyl ligand was disordered over the two orientations in an approximate 50:50 ratio. In one part of the disorder (A in Fig. 3) the terminal allyl C atoms are atoms C21A and C22A, and the methyl group is C23A, while the central pivotal allylic carbon atom is labeled C20A; in the other part (B in Fig. 3) these atoms become C24B, C25B, C26B and C20B, respectively.

3. Conclusions

New 2-Me-allylpalladium derivatives with bis(pyrazol-1-yl)methane or bis(3,5-dimethylpyrazol-1-yl)methane ligands bearing a substituent in the methylenic spacer group, R, have been prepared and char-

acterized. These complexes have two isomeric forms in solution (*endo* and *exo*) that differ in the orientation of the allyl ligand. NOE experiments have shown that the N,N-donor ligands exist in a rigid boat conformation in solution with the R group in an axial position with respect to the PdNNCNN metallacycle. VT NMR analysis has demonstrated that, in the temperature range studied, the R group is in a free rotation regime when R is a phenylic group whereas it has a restricted rotation when the R group is Cy or Fc. The isomers are in equilibrium and their interconversion by an apparent allyl rotation has been studied on the NMR time scale. On the basis of the $\Delta G_c^{\ddagger}$ values obtained, the mechanism proposed for this isomerization implies the occurrence of a counteranion–cation contact through pentacoordinate intermediates. These contacts are more difficult to achieve when bulky groups (R or pyrazole substituents) are present. In accordance with this mechanism, dilution or addition of Cl^- to a solution of one of the complexes produced the expected increase or decrease, respectively, in the $\Delta G_c^{\ddagger}$ values.

4. Experimental

4.1. Starting materials and general conditions

4.1.1. General comments

All manipulations were carried out under an atmosphere of dry oxygen-free nitrogen using standard Schlenk techniques. Solvents were distilled from the appropriate drying agents and degassed before use. AgTfO was used as purchased from Aldrich. The preparation of the ligands bpzmArOH and bpz*mArOH has been previously reported [18]. The preparation of the rest of the ligands has been recently described by us [13a]. $[Pd_2(\eta^3\text{-}2\text{-}Me\text{-}C_3H_4)_2(\mu\text{-}Cl)_2]$ was prepared as described in the literature [19]. Elemental analyses were performed with a Thermo Quest FlashEA 1112 microanalyzer. IR spectra were recorded as KBr pellets with a Perkin–Elmer PE 883 IR spectrometer. ^1H and ^{13}C spectra were recorded on a VARIAN UNITY 300 spectrometer. Chemical shifts (ppm) are given relative to Me_4Si. COSY spectra: standard pulse sequence with an acquisition time of 0.214 s, pulse width 10 ms, relaxation delay 1 s, number of scans 16, number of increments 512. The NOE difference spectra were recorded with the following acquisition parameters: spectral width 5000 Hz, acquisition time 3.27 s, pulse width 18 ms, relaxation delay 4 s, irradiation power 5–10 dB, number of scans 240. For variable temperature spectra the probe temperature (± 1 K) was controlled by a standard unit calibrated with a methanol reference. Free energies of activation (kJ mol^{-1}) were calculated [20] from the coalescence temperature (T_c) and the frequency difference between the coalescing signals (extrapolated at the coalescence temperature) according with the Shanan–Atidi and Bar–Eli [21] method with the formula $\Delta G_c^{\ddagger} = aT[10.319 + \log(T/\kappa)]$, $a = 1.914 \times 10^{-2}$. The estimated error in the calculated free energies of activation is ± 1.0 kJ mol^{-1}. *M* and *m* refers to the major or minor isomers, respectively.

4.1.2. X-ray structural determination of 2 and 5

2. A suitable crystal of **2** was mounted under a stream of cold N_2 on a Siemens SMART diffractometer fitted with a CCD-type area detector. A hemisphere of data was collected at low temperature using graphite monochromated Mo–K_α radiation. A detailed experimental description of the methods used for data collection and integration using the SMART system has been published [22]. Empirical absorption corrections were applied using SADABS [23], and structure solution and refinement was performed with the SHELX suite of programs [24]. The crystal of **2** was stable and diffracted well and the structure was solved by direct methods.

5. A suitable crystal was selected and mounted on fine glass fibbers with epoxy cement. Accurate unit-cell parameters were derived from the least-squares fit of the angular setting of 25 high-order reflections. The data collection was performed on a Nonius-Mach3 diffractometer equipped with a graphite monochromated Mo–K_α radiation ($\lambda = 0.71070$ Å) using a ω–2θ scan technique to a θ maximum value of 28°. The compound crystallizes in the orthorhombic group *Pnma* with half molecule of **5** per asymmetric unit, $Z = 4$. Parameters for the collection and refinement of diffraction data are contained in Table 4. Intensities were corrected for Lorentz and polarization effects and absorption correction was not necessary.

The structure was solved using direct methods [25] and refined first isotropically by full-matrix least-squares using SHELXL-97 [26] program and then anisotropically by blocked full-matrix least-squares for all the non-hydrogen atoms. The hydrogen atoms were included in calculated positions and were refined isotropically.

4.2. Preparations

4.2.1. [Pd(η³-C4H7)(bpzmArOH)]TfO (1)

To a solution of $[Pd(\eta^3\text{-}C_4H_7)(\mu\text{-}Cl)]_2$ (100 mg, 0.25 mmol) in 20 ml of acetone, AgTfO (128 mg, 0.5 mmol) was added. The solution was stirred at r.t. for 1 h and the resulting suspension was filtered off. Then bpzmArOH (120 mg, 0.5 mmol) was added to the filtrate. After stirring for 1 h, the solution thus formed was evaporated to dryness. The resulting white solid was washed with diethyl ether (2×20 ml). White crystals were obtained after a recrystallization from acetone–diethyl ether. Yield: 55%. $C_{18}H_{19}F_3N_4O_4PdS$ (550.79): Calc. C, 39.25; H, 3.48; N, 10.17; S, 5.82. Found: C,

38.99; H, 3.70; N, 9.94; S, 5.94%. IR (cm^{-1}, KBr): 1519 (C=Npz); 3266 (ν OH); 1314, 1034, 795, 639 (CF_3SO_3), 1385, 832 (2-Me-C_3H_4).

4.2.2. [Pd(η^3-C_4H_7)(bpzmArOMe)]TfO (2)

A similar procedure to that used for **1** was followed for **2**. The amount of ligand bpzmArOMe added was 127 mg (0.5 mmol). Yield: 50%. $C_{19}H_{21}F_3N_4O_4PdS$ (564.87): Calc. C, 40.40; H, 3.75; N, 9.92; S, 5.68. Found: C, 39.98; H, 3.76; N, 9.64; S, 5.67%. IR (cm^{-1}, KBr): 1585 (C=Npz); 1143 (ν_{as} C–O–C); 1302, 1018, 784, 635 (CF_3SO_3), 1374, 837 (2-Me-C_3H_4).

4.2.3. [Pd(η^3-C_4H_7)(bpz*mArOH)]TfO (3)

A similar procedure to that used for **1** was followed for **3**. The amount of ligand bpz*mArOH added was 148 mg (0.5 mmol). Yield: 55%. $C_{22}H_{27}F_3N_4O_4PdS$ (606.95): Calc. C, 43.54; H, 4.48; N, 9.23; S, 5.28. Found: C, 43.87; H, 4.61; N, 8.94; S, 4.98%. IR (cm^{-1}, KBr): 1557 (C=Npz); 3255 (ν OH); 1047, 803, 638 (CF_3SO_3); 1374, 842 (2-Me-C_3H_4).

4.2.4. [Pd(η^3-C_4H_7)(bpz*mArOMe)]TfO·1/2C_3H_6O (4)

A similar procedure to that used for **1** was followed for **4**. The amount of ligand bpz*mArOMe added was 155 mg (0.5 mmol). The recrystallization was made from acetone–diethyl ether. Yield: 80%. $C_{23}H_{29}F_3N_4O_4PdS\cdot 1/2C_3H_6O$ (621.93): Calc. C, 44.48; H, 4.71; N, 9.02; S, 5.16. Found: C, 44.23; H, 4.49; N, 8.88; S, 4.70%. IR (cm^{-1}, KBr): 1557 (C=Npz); 1143 (ν_{as} C–O–C); 1321, 1048, 789, 636 (CF_3SO_3); 1390, 842 (2-Me-C_3H_4).

4.2.5. [Pd(η^3-C_4H_7)(bpz*mCy)]TfO (5)

A similar procedure to that used for **1** was followed for **5**. The amount of ligand bpz*mCy added was 143 mg (0.5 mmol). The recrystallization was made from 1,2-dichloroetane–pentane. Suitable white crystals for X-ray diffraction were obtained. Yield: 92%. $C_{22}H_{33}F_3N_4O_3PdS$ (698.86): Calc. C, 44.26; H, 5.57; N, 9.38; S, 5.37. Found: C, 44.09; H, 5.48; N, 9.68; S, 5.29%. IR (cm^{-1}, KBr): 1559 (C=Npz); 1269, 1144, 637 (CF_3SO_3); 1392, 837 (2-Me-C_3H_4).

4.2.6. [Pd(η^3-C_4H_7) (bpz*mFc)]TfO (6)

A similar procedure to that used for **1** was followed for **6**. The amount of ligand bpz*mFc added was 194 mg (0.5 mmol). The recrystallization was made from acetone–diethyl ether, giving yellow crystals. Yield: 74%. $C_{26}H_{31}F_3FeN_4O_3PdS$ (698.86): Calc. C, 44.69; H, 4.47; N, 8.02; S, 4.59. Found: C, 44.86; H, 4.54; N, 8.06; S, 4.47%. IR (cm^{-1}) (KBr): 1559 (C=Npz); 819 (π CH, Fc); 1263, 1148, 636 (CF_3SO_3); 1392, 837 (2-Me-C_3H_4).

4.2.7. NMR determination of Tc

0.5 ml of a solution of known concentration (1.3–1.9×10^{-2} mol l^{-1}) of complexes **2** or **4**–**7** in 1,1′,2,2′-tetrachloroethane-d_2 was introduced into a 5 mm NMR tube. The temperature of the probe was decreased to −20 °C (253 K). NMR spectra were recorded as the temperature was increased at intervals of 5 °C, with a stabilization time of 10 min between each measurement. The spectra were acquired at intervals of only 1 or 2° near the coalescence temperature. For complex **4** the coalescence temperatures were calculated on a 1.6×10^{-2} mol l^{-1} solution (0.5 ml, 0.8×10^{-2} mmol). Additional deuterated solvent (0.25 ml) was added to 0.25 ml of the above solution in order to obtain the diluted sample. Another solution was prepared by adding 5.14 mg of PPh_4Cl (1.37×10^{-2} mmol) to 0.50 ml of a 1.6×10^{-2} mol l^{-1} solution of complex **4** in 1,1′,2,2′-tetrachloroethane-d_2 (ratio Cl^-/**4** = 1.7). In all the solutions the coalescence temperatures were then measured by the standard method.

5. Supplementary material

Crystallographic data for the structural analysis have been deposited at the Cambridge Crystallographic Data Centre, and allocated the deposition numbers CCDC no. 174713 for **2** and 174714 for **5**. Copies of this information may be obtained free of charge from The Director, CCDC, 12 Union Road, Cambridge CB2 1EZ, UK (Fax: +44-1223-336033; or e-mail: deposit@ccdc.a-c.uk or http://www.ccdc.cam.ac.uk).

Acknowledgements

We gratefully acknowledge financial support from the Dirección General de Investigación Científica y Técnica (DGICyT) (Grant no. PB98-0315) of Spain and the "Junta de Comunidades de Castilla-La Mancha" for a grant (to A.G.).

References

[1] (a) J. Tsuji, Palladium Reagents and Catalysts, Innovation in Organic Synthesis, Wiley, Chichester, 1996;
(b) B.M. Trost, Pure Appl. Chem. 68 (1996) 779;
(c) C. Bolm, D. Kaufmann, M. Zehnder, M. Neuburger, Tetrahedron Lett. 37 (1996) 3985;
(d) J.D. Oslob, B. Åkermark, P. Helquist, P.O. Norrby, Organometallics 16 (1997) 3015;
(e) C. Larksarp, H. Alper, J. Am. Chem. Soc. 119 (1997) 3709;
(f) H. Hagelin, B. Åkermark, P.-O. Norrby, Organometallics 18 (1999) 2884;
(g) J.C. Anderson, R.J. Cubbon, J.D. Harling, Tetrahedron Asymmetry 10 (1999) 2829;
(h) E. Adams, J.C. Anderson, R. Cubbon, D.S. James, J.P.

Mathias, J. Org. Chem. 52 (1999) 8255;
(i) M. Sauthier, J. Fornies-Camer, L. Toupet, R. Réau, Organometallics 19 (2000) 553;
(j) J.M. Canal, M. Gómez, F. Jiménez, M. Rocamora, G. Muller, E. Dunach, D. Franco, A. Jiménez, F.H. Cano, Organometallics 19 (2000) 955;
(k) L. Barloy, S. Ramdeehul, J.A. Osborn, C. Carlotti, F. Taulelle, A. De Cian, J. Fischer, Eur. J. Inorg. Chem. 12 (2000) 2523;
(l) U. Nettekoven, M. Widhalm, H. Kalchhauser, P.C.J. Kamer, P.W.N.M. van Leeuwen, M. Lutz, A.L. Spek, M. Wildham, J. Org. Chem. 66 (2001) 759;
(m) J.C. Anderson, R.J. Cubbon, J.D. Harling, Tetrahedron Asymmetry 12 (2001) 923.

[2] (a) K. Vrieze, in: L.M. Jackman, F.A. Cotton (Eds.), Dynamic Nuclear Resonance Spectroscopy, Academic Press, New York, 1975;
(b) P.S. Pregosin, R. Salzmann, Coord. Chem. Rev. 155 (1996) 35;
(c) F.A. Jalón, B.R. Manzano, F. Gómez-de la Torre, A.M. Guerrero, A.M. Rodríguez, in: O.A. Attanasi, D. Spinelli (Eds.), Targets in Heterocyclic Systems, Chemistry and Properties, vol. 3, Italian Society of Chemistry, Rome, 1999, p. 399.

[3] P.W.N.M. van Leeuwen, P.W. Praat, J. Chem. Soc. Chem. Commun. (1970) 365.

[4] (a) J.M. Brown, D.I. Hulmes, P.J. Guiry, Tetrahedron 50 (1994) 4493;
(b) R. Fernández-Galán, F. Jalón, B.R. Manzano, J. Rodríguez de la Fuente, M. Vrahami, B. Jedlicka, W. Weissensteiner, Organometallics 16 (1997) 3758;
(c) T.D.W. Claridge, J.M. Long, J.M. Brown, D. Hibbs, M.B. Hursthouse, Tetrahedron 53 (1997) 4035.

[5] (a) G.L. Statton, K.C. Ramey, J. Am. Chem. Soc. 88 (1966) 4387;
(b) J.S. Lippard, S.M. Morehouse, J. Am. Chem. Soc. 94 (1972) 6949;
(c) C. Breutel, P.S. Pregosin, R. Salzmann, A. Togni, J. Am. Chem. Soc. 116 (1994) 4067;
(d) C. Breutel, P.S. Pregosin, R. Salzmann, A. Togni, J. Am. Chem. Soc. 116 (1994) 4067;
(e) P.S. Pregosin, R. Salzmann, A. Togni, Organometallics 14 (1995) 842;
(f) J. Herrmann, P.S. Pregosin, R. Salzmann, Organometallics 14 (1995) 3311;
(g) T. Hosocawa, Y. Wakabayashi, K. Hosocawa, T. Tsuji, S.I. Murahashi, J. Chem. Soc. Chem. Commun. (1996) 859.

[6] F.G.A. Stone, N.M. Boag, M. Green, J.L. Spencer, J. Organomet. Chem. 127 (1977) C51.

[7] (a) R.E. Rülke, V.E. Raasjager, P. Wehman, C.J. Elsevier, P.W.N.M. van Leeuwen, K. Vrieze, J. Fraanje, K. Boubitz, A.L. Spek, Organometallics 15 (1996) 3022;
(b) F. Gómez-de la Torre, Y. Gutiérrez, F.A. Jalón, B.R. Manzano, A. Rodríguez, Monatsh. Chem. 131 (2000) 1267;
(c) S. Ramdeehul, L. Barloy, J.A. Orborn, A. De Cian, J. Fischer, Organometallics 15 (1996) 5442;
(d) H.A. Ankersmit, N. Veldman, A.L. Spek, K. Vrieze, G. Van Koten, Inorg. Chim. Acta 252 (1996) 339;
(e) L. Canovese, F. Visentin, P. Uguabliati, G. Chessa, V. Lucchini, G. Bandoli, Inorg. Chim. Acta 1–2 (1998) 385;
(f) P. Braunstein, F. Naud, A. Dedieu, M.M. Rohmer, A. De Cian, S.J. Rettig, Organometallics 14 (2001) 2966.

[8] (a) F.A. Jalón, B.R. Manzano, A. Otero, M.C. Rodríguez, J. Organomet. Chem. 494 (1995) 179;
(b) J. Elguero, A. Fruchier, A. de la Hoz, F.A. Jalón, B.R. Manzano, A. Otero, F. Gómez-de la Torre, Chem. Ber. 129 (1996) 589;
(c) J.G.P. Delis, J.H. Groeen, K. Vrieze, P.W.N.M. van Leeuwen, N. Veldman, A.L. Spek, Organometallics 16 (1997) 551;
(d) F. Gómez-de la Torre, A. de la Hoz, F.A. Jalón, B.R. Manzano, A. Otero, A.M. Rodríguez, M.C. Rodríguez-Pérez, A. Echevarría, J. Elguero, Inorg. Chem. 37 (1998) 6606;
(e) Y. Takao, T. Takeda, J. Watanabe, J. Setsune, Organometallics 18 (1999) 2936;
(f) F. Gómez-de la Torre, A. de la Hoz, F.A. Jalón, B.R. Manzano, A.M. Rodríguez, J. Elguero, M. Martínez-Ripoll, Inorg. Chem. 39 (2000) 1152;
(g) N. Arroyo, F. Gómez-de la Torre, F.A. Jalón, B.R. Manzano, B. Moreno-Lara, A.M. Rodríguez, J. Organomet. Chem. 603 (2000) 174.

[9] (a) B. Crociani, F. Di Bianca, A. Giovenco, T. Bozchi, Inorg. Chim. Acta 127 (1987) 169;
(b) S. Hansson, P.O. Norrby, M.P.T. Sjögren, B. Åkermark, M.E. Cucciolito, F. Giorjano, A. Vitagliano, Organometallics 12 (1993) 4949;
(c) B. Crociani, S. Antonaroli, M. Paci, F. Di Bianca, L. Canovese, Organometallics 16 (1997) 384.

[10] (a) A. Albinati, R.W. Kunz, C.J. Ammann, P.S. Pregosin, Organometallics 10 (1991) 1800;
(b) A. Gogoll, J. Örnebro, J.-E. Bäckvall, J. Am. Chem. Soc. 116 (1994) 3631;
(c) A. Gogoll, H. Grennberg, A. Axén, Organometallics 16 (1997) 1167.

[11] P.K. Byers, A.J. Canty, R.T. Honeyman, Adv. Organomet. Chem. 34 (1992) 1.

[12] (a) D.G. Brown, P.K. Byers, A. Canty, Organometallics 9 (1990) 1231;
(b) G. Minghetti, M.A. Cinellu, A.B.G. Banditelli, F. Demartin, M. Manassero, J. Organomet. Chem. 315 (1986) 387;
(c) P.K. Byers, A.J. Canty, Organometallics 9 (1990) 210.

[13] (a) M.C. Carrión, A. Díaz, A. Guerrero, F.A. Jalón, B.R. Manzano, A. Rodríguez, New J. Chem. (2002), in press;
(b) P.K. Byers, A.J. Canty, R.T. Honeyman, J. Organomet. Chem. 385 (1990) 417;
(c) P.K. Byers, A.J. Canty, Organometallics 9 (1990) 210.

[14] (a) K.I. Thé, L.K. Peterson, Can. J. Chem. 51 (1973) 422;
(b) K.I. Thé, L.K. Peterson, E. Kiehlmann, Can. J. Chem. 51 (1973) 2448;
(c) L.K. Peterson, E. Kiehlmann, A.R. Sanger, K.I. Thé, Can. J. Chem. 52 (1974) 2367.

[15] S. Trofimenko, Scorpionates, The Coordination Chemistry of Polypyrazolylborate Ligands, Imperian College Press, London, 1999.

[16] (a) M.A. Kennedy, P.D. Ellis, Inorg. Chem. 29 (1990) 541;
(b) L. Komorowski, A. Meller, K. Niedenzu, Inorg. Chem. 29 (1990) 538;
(c) D.G. Brown, P.K. Byers, A. Canty, Organometallics 9 (1990) 1231;
(d) K. Niedenzu, J. Serwatowski, S. Trofimenko, Inorg. Chem. 30 (1991) 524.

[17] (a) S. Tsuji, D.C. Swenson, R.F. Jordan, Organometallics 18 (1999) 4758;
(b) G. Minghetti, M.A. Cinellu, A.B.G. Banditelli, F. Demartin, M. Manassero, J. Organomet. Chem. 315 (1986) 387;
(c) A.J. Canty, N.J. Minchin, L.M. Engelhardt, B.W. Sketton, A.H. While, J. Chem. Soc. Dalton Trans. (1986) 645.

[18] T.C. Higgs, C.J. Carrano, Inorg. Chem. 36 (1997) 298.

[19] (a) W.T. Dent, R. Long, G. Wilkinson, J. Chem. Soc. (1964) 1585.;
(b) Y. Tatsuno, T. Yoshida, Seiotsuha, Inorg. Synth. 19 (1979) 220.

[20] J. Sandström, Dynamic NMR Spectroscopy, Academic Press, London, 1982.

[21] H. Shanan-Atidi, K.H. Bar-Eli, J. Phys. Chem. 74 (1970) 961.

[22] P.L. Jones, A.J. Amoroso, J.C. Jeffery, J.A. McCleverty, E. Psillakis, L.H. Rees, M.D. Ward, Inorg. Chem. 36 (1997) 10; SMART and SAINT, Area-Detector Control and Integration Soft-

ware, Siemens Analytical X-Ray Instruments Inc., Madison WI, 1995.
[23] SADABS, a program for absorption correction with the Siemens SMART area-detector system, G.M. Sheldrick, University of Göttingen, 1996.
[24] SHELXTL 5.1 program system, Siemens Analytical X-Ray Instruments, Madison, WI, 1998.
[25] A. Altomare, G. Cascarano, C. Giacovazzo, A. Guagliardi, M.C. Burla, G. Polidori, M. Camalli, J. Appl. Cryst. (1994) 435.
[26] G.M. Sheldrick, Program for the Refinement of Crystal Structures from Diffraction data, University of Göttingen, Göttingen, Germany, 1997.